Postbuckling of Long Orthotropic Plates Under Combined Loading

Manuel Stein*
NASA Langley Research Center, Hampton, Virginia

The postbuckling behavior of simply supported, rectangular, isotropic, and orthotropic composite plates under combined loading is determined analytically. Results are presented for a long plate loaded beyond its buckling load in either a combination of longitudinal and transverse compression or a combination of transverse compression and inplane shear. Results show that orthotropic plates may behave differently than isotropic plates for these loading conditions. Results also show that the postbuckling behavior of plates in shear with constrained edge displacements is markedly different than their behavior with stress free edges.

Nomenclature

$A_{11}, A_{22}, A_{12}, A_{66}$ = orthotropic plate extensional stiffnesses
a, b = dimensions of rectangular plate parallel to x and y axes, respectively
$D_{11}, D_{22}, D_{12}, D_{66}$ = orthotropic plate bending stiffnesses
M_x, M_y, M_{xy}, N_x, N_y, N_{xy} = bending moments in plate, inplane stress resultants in plate
$N_{xav}, N_{yav}, N_{xyav}$ = average value of stress resultants, see Eqs. (5)
$N_{xcr}, N_{ycr}, N_{xycr}$ = buckling value of stress resultants for simply supported long plate
$N_{xcr}b^2/(\sqrt{D_{11}D_{22}}\pi^2)$ = $\begin{cases} 4, \text{ isotropic plate} \\ 6.56, \pm 45^\circ \text{ composite plate} \end{cases}$
$N_{ycr}b^2/(D_{22}\pi^2)$ = $\begin{cases} 1, \text{ isotropic plate} \\ 1, \pm 45^\circ \text{ composite plate} \end{cases}$
$N_{xycr}b^2/(\sqrt[4]{D_{11}D_{22}^3}\pi^2)$ = $\begin{cases} 5.33, \text{ isotropic plate} \\ 7.41, \pm 45^\circ \text{ composite plate} \end{cases}$
u, v = displacements in x and y directions, respectively
$\bar{u}, \bar{v}, \bar{u}_{sh}$ = applied compressive displacements in x and y directions, respectively, and applied shear displacement
$\bar{u}_{cr}, \bar{v}_{cr}, \bar{u}_{shcr}$ = buckling values of the applied displacements
$\bar{u}_{cr}$ = $aN_{xcr}/(A_{11} - A_{12}^2/A_{22})$
$\bar{v}_{cr}$ = $bN_{ycr}/(A_{22} - A_{12}^2/A_{11})$
$\bar{u}_{shcr}$ = bN_{xycr}/A_{66}
$u_0, u_s, u_c, v_0, v_s, v_c$ = arbitrary functions of y appearing in Eq. (1) for u and v
w = deflection normal to the plate
w_s, w_c = arbitrary functions of y appearing in Eq. (1) for w
x, y = plate coordinates
$\epsilon_x, \epsilon_y, \gamma_{xy}$ = neutral surface strains in plate
$\kappa_x, \kappa_y, \kappa_{xy}$ = curvatures in plate
λ = half-wavelength of plate deflection

Introduction

ONE of the basic elements in a structure is the rectangular flat plate supported at its edges. An orthotropic plate may be constructed to have various extensional and bending properties. Design methods need to be established for orthotropic plates for a variety of structural configurations and loadings. Because a structure is often subjected to combinations of loads, attention has been given to the problem of buckling of plates when more than one type of loading is present. In Refs. 1-3, combinations of loading were considered for buckling, and it was shown that it is convenient to draw interaction curves giving critical combinations of loading.

Supported plates, unlike columns and many types of shells, may carry considerable load beyond buckling. In the design of aerospace structures, it is advantageous to permit the plate to be loaded elastically into the postbuckling range. Its load carrying ability beyond buckling is of interest. Postbuckling behavior can be obtained for many plate configurations using a general purpose computer program such as that described in Ref. 4. However, use of a special purpose program to calculate the behavior for a variety of combinations of loadings and plate materials may be more economically feasible.

A special purpose program has been developed for the postbuckling of orthotropic composite plates loaded in compression.[5] This program was extended for shear of long orthotropic composite plates and for combined shear and longitudinal compression[6] and was then modified to allow specification of the inplane transverse displacement of the long edges.[7]

The special purpose program of Ref. 7 is more efficient than available general purpose programs that might do the same calculations and is used to obtain the results in the present paper. This program is based on the nonlinear partial differential plate equations of von Kármán. These equations are transformed into nonlinear ordinary differential equations by assuming trigonometric functions in one of the plate coordinate directions. The transformed equations are then solved numerically using the method of Ref. 8. The effects of change in buckle pattern are included in the calculations.

Analysis

The analysis used to obtain the results of the present paper was derived in Ref. 7. In the present paper, trigonometric approximations for displacements, the strain-displacement and stress-strain laws, and virtual work of the systems used to derive the ordinary differential equations are given. The ordinary differential equations are written as a set of first-

Received April 10, 1984; presented as Paper 84-0890 at the AIAA/ASME/ASCE/AHS 25th Structures, Structural Dynamics and Materials Conference, Palm Springs, Calif., May 14-16,1984; revision received Sept. 21, 1984. This paper is declared a work of the U.S. Government and therefore is in the public domain.

*Senior Aerospace Engineer, Structural Mechanics Branch, Structures and Dynamics Division. Associate Fellow AIAA.

order differential equations which can be solved in conjunction with the boundary conditions using an algorithm based on Newton's method. Meaningful results are obtained when the solution is along the desired equilibrium path and the wavelength is chosen to give minimum total potential energy. The loading is effected by prescribing displacements $\bar{u}$, $\bar{v}$, $\bar{u}_{sh}$ as discussed in the following paragraph.

A buckled plate loaded by combined longitudinal and transverse compression is shown in Fig. 1a, and a buckled plate loaded in transverse compression and shear is shown in Fig. 1b. The plates have a width b and a half-wavelength λ in the y and x directions, respectively. For the longitudinal compression loading, displacements $\bar{u}/2$ are applied at the ends of the plate. To achieve a combined loading, $\bar{u}$ is specified for longitudinal compressive loading, $\bar{v}$ is specified for transverse compressive loading, and $\bar{u}_{sh}$ is specified for shear loading. The out-of-plane deflection w is zero at the nodal lines of the buckle pattern (every half-wavelength), and w is zero at the edges $y=0$, b.

Displacements

Nonlinear ordinary differential equations are derived based on a trigonometric series approximation for the displacements. The selection of the terms in the trigonometric series are based on the exact terms required for prebuckling and buckling and a few terms beyond as suggested by a perturbation method (see, for example, Ref. 9). The terms selected for the displacements form the right-hand side of the equations which follow. They are appropriate for compression, for shear, and for a combination of compression and shear (see Ref. 6).

$$u = -\bar{u}\left(\frac{x}{a}-\frac{1}{2}\right) + u_0(y) + u_s(y)\sin\frac{2\pi x}{\lambda} + u_c(y)\cos\frac{2\pi x}{\lambda}$$

$$v = v_0(y) + v_s(y)\sin\frac{2\pi x}{\lambda} + v_c(y)\cos\frac{2\pi x}{\lambda}$$

$$w = w_s(y)\sin\frac{\pi x}{\lambda} + w_c(y)\cos\frac{\pi x}{\lambda} \qquad (1)$$

The deflection w, which is exact at buckling, is sinusoidally periodic with half-wavelength λ. The displacements u and v are sinusoidally periodic with half-wavelengths $\lambda/2$, and u has an extra, linear-in-x term associated with the constant $\bar{u}$ which is specified. Specifying $\bar{u}$ identifies the applied longitudinal compressive displacement. The applied shearing displacement $\bar{u}_{sh}$ is specified through boundary conditions on $u_0(y)$. The applied transverse compressive displacement is specified through boundary conditions on $v_o(y)$.

Derivation of Differential Equations

The neutral surface strains and curvatures as given by von Kármán are

$$\epsilon_x = u_{,x} + \tfrac{1}{2}w_{,x}^2 \qquad \kappa_x = -w_{,xx}$$

$$\epsilon_y = v_{,y} + \tfrac{1}{2}w_{,y}^2 \qquad \kappa_y = -w_{,yy}$$

$$\gamma_{xy} = u_{,y} + v_{,x} + w_{,x}w_{,y} \qquad \kappa_{xy} = -2w_{,xy} \qquad (2)$$

From the stress-strain relations for an orthotropic plate, the stress and moment resultants are

$$N_x = A_{11}\epsilon_x + A_{12}\epsilon_y \qquad M_x = D_{11}\kappa_x + D_{12}\kappa_y$$

$$N_y = A_{22}\epsilon_y + A_{12}\epsilon_x \qquad M_y = D_{22}\kappa_y + D_{12}\kappa_x$$

$$N_{xy} = A_{66}\gamma_{xy} \qquad M_{xy} = D_{66}\kappa_{xy} \qquad (3)$$

The virtual work of the system is

$$\delta\Pi = \int_0^b\int_0^\lambda (N_x\delta\epsilon_x + N_y\delta\epsilon_y + N_{xy}\delta\gamma_{xy} + M_x\delta\kappa_x + M_y\delta\kappa_y + M_{xy}\delta\kappa_{xy})\,dx\,dy \qquad (4)$$

From basic relations (2-4) and simplifying assumption (1), nonlinear ordinary differential equations have been derived in Ref. 7 to replace the nonlinear partial differential equations of plate theory.

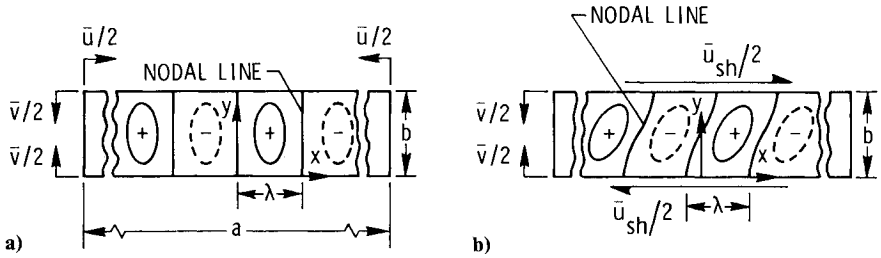

Fig. 1 Long plate a) buckled by combined longitudinal and transverse compression and b) buckled in transverse compression and shear.

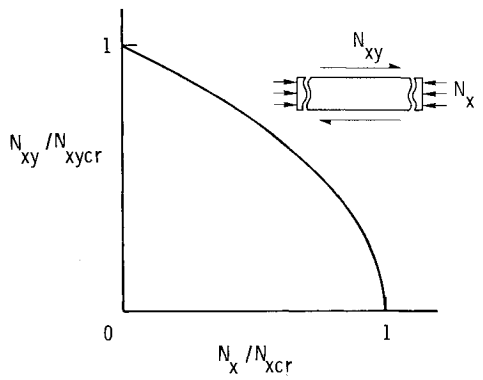

Fig. 2 Combinations of shear and longitudinal compression for buckling of a long plate.[1]

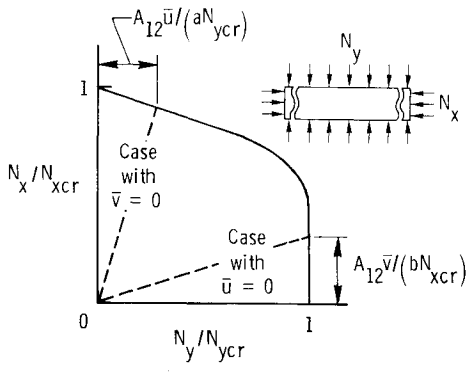

Fig. 3 Combinations of longitudinal and transverse compression for buckling of a long plate.[2]

Boundary Conditions

The boundary conditions assumed for the results presented herein are that the edges are simply supported and held straight. The edges are simply supported if $w=0$ and $M_y=0$ at $y=0$, b. The edges are held straight if, at $y=0$, b, $u_s=u_c=v_s=v_c=0$. The applied displacements are given by $\bar{u}$ for longitudinal compression, by $v_0=\bar{v}/2$ at $y=0$ and $v_0=-\bar{v}/2$ at $y=b$ for transverse compression, and by $u_0=-\bar{u}_{sh}/2$ at $y=0$ and $u_0=\bar{u}_{sh}/2$ at $y=b$ for shear.

Solution Technique

Solution of the ordinary differential equations, subject to the specified boundary conditions, is obtained using an algorithm based on Newton's method developed by Lentini and Pereyra in Ref. 8. This algorithm solves a system of simultaneous first-order nonlinear ordinary-differential equations subject to two point boundary conditions. The system of equations has the form $\bar{U}'=\bar{F}(y,\bar{U})$, where $\bar{U}2$ is the vector of dependent variables and y the independent variable defined in the interval $(0,b)$. The boundary conditions of the problem are specified by $\bar{g}[\bar{U}(0),\ \bar{U}(b)]=0$. This algorithm uses finite differences with deferred corrections, and adaptive mesh spacings are automatically produced so that mild boundary layers are detected and resolved.

Applications

This paper presents results for a long plate loaded beyond its buckling load in either a combination of longitudinal and transverse compression or in a combination of transverse compression and inplane shear. For given values of the applied displacements $\bar{u}$, $\bar{v}$, and $\bar{u}_{sh}$, and for prescribed values of the dimensions, material properties, and half-wavelength λ, the system of equations is solved and the average compressive-stress resultants and shear-stress resultants are determined, where the average stress resultants are

$$N_{xav}=-\frac{1}{2b\lambda}\int_0^b\int_0^{2\lambda}N_x\,dx\,dy$$

$$N_{yav}=-\frac{1}{2b\lambda}\int_0^b\int_0^{2\lambda}N_y\,dx\,dy$$

$$N_{xyav}=\frac{1}{2b\lambda}\int_0^b\int_0^{2\lambda}N_{xy}\,dx\,dy \qquad (5)$$

The solution of interest is on an equilibrium path that gives nonzero deflections, and the wavelength of interest is the one that corresponds to minimum total potential energy.

Results are obtained for isotropic and ±45° laminated composite plates with a balanced and symmetric layup. The isotropic results apply to isotropic metal plates or composite plates with a quasi-isotropic layup. The ±45° laminate results apply to graphite-epoxy filamentary material with properties given by the dimensionless quantities

$$\frac{D_{12}+2D_{66}}{\sqrt{D_{11}D_{22}}}=2.28$$

$$\frac{A_{11}A_{22}-A_{12}^2-2A_{12}A_{66}}{2A_{66}\sqrt{A_{11}A_{22}}}=-0.431$$

For the isotropic plate both of these quantities are unity, and for both the isotropic and the ±45° laminate

$$A_{22}D_{11}/A_{11}D_{22}=1$$

As discussed in Ref. 5, the three dimensionless quantities just shown may be used to present postbuckling results with a minimum number of parameters.

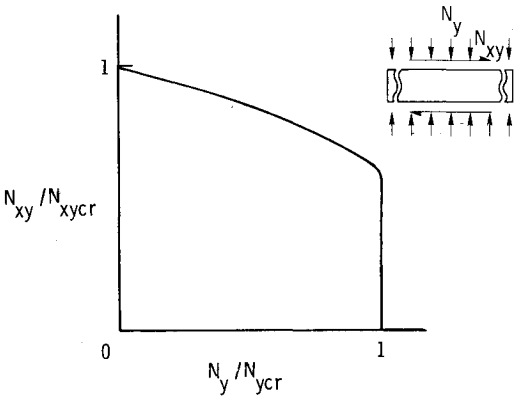

Fig. 4 Combinations of shear and transverse compression for buckling of a long plate.[3]

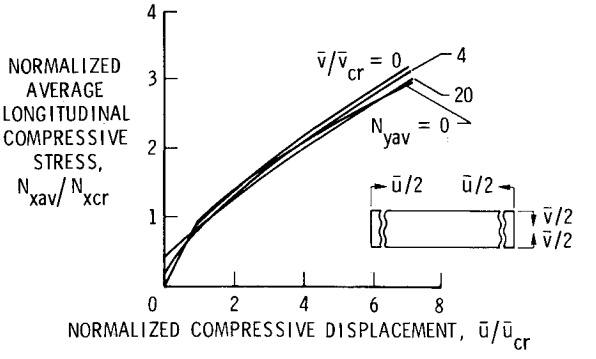

Fig. 5 Average longitudinal compressive stress for a long isotropic plate in combined longitudinal and transverse compression.

Results and Discussion

Buckling results for long plates in combined longitudinal compression and shear were obtained in Ref. 1. The interaction curve for isotropic and orthotropic plates buckling under this combined loading is given by a simple parabola as shown in Fig. 2. Postbuckling results are presented for long isotropic and orthotropic plates in combined longitudinal compression and shear in Ref. 6. Postbuckling results are presented in Ref. 6 by two sets of curves with different loading parameters held constant. In one set of curves, the compressive displacement representing the abscissa in Fig. 2 is held constant and in the other set of curves the shear displacement representing the ordinate in Fig. 2 is held constant.

The interaction curve for buckling of a long plate in combined longitudinal and transverse compression was obtained in Ref. 2 and is presented in Fig. 3. The curve has discontinuous curvature and a vertical line at the right. The wavelength becomes large, and cylindrical bending occurs for the results in this region of the interaction curve. The interaction curve for buckling of a long plate in combined transverse compression and shear was obtained in Ref. 3 and is presented in Fig. 4. Again, the curve has discontinuous curvature and a vertical line at the right that occurs when the wavelength becomes large and cylindrical bending occurs.

Combined Longitudinal and Transverse Compression

The average longitudinal stress resultant N_{xav} of a long plate loaded in combinations of applied compressive longitudinal and transverse displacements $\bar{u}$ and $\bar{v}$, respectively, is given in Fig. 5 for an isotropic plate. N_{xav} is plotted vs $\bar{u}$ for different values of $\bar{v}$. A similar plot is shown in Fig. 6 for a ±45° laminated composite plate. In the figures, N_{xav} is normalized by N_{xcr}, the stress resultant at buckling when

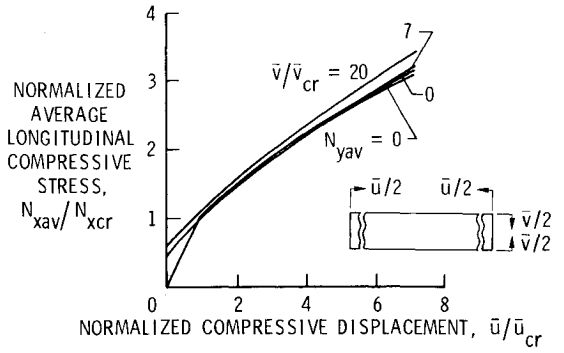

Fig. 6 Average longitudinal compressive stress for a long ±45° laminated composite plate in combined longitudinal and transverse compression.

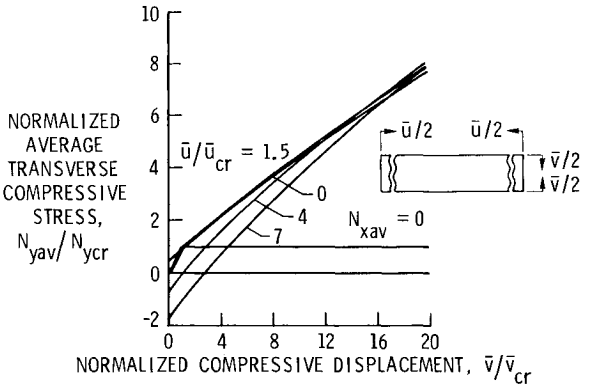

Fig. 7 Average transverse compressive stress for a long isotropic plate in combined longitudinal and transverse compression.

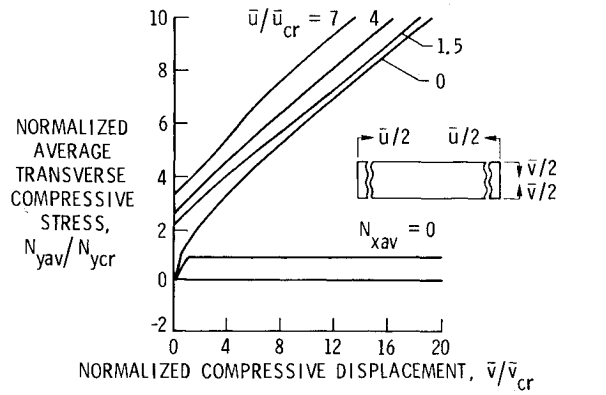

Fig. 8 Average transverse compressive stress for a long ±45° laminated composite plate in combined longitudinal and transverse compression.

only N_x is acting, and $\bar{u}$ and $\bar{v}$ are normalized by the corresponding displacements at buckling $\bar{u}_{cr}$ and $\bar{v}_{cr}$. The $\bar{v}=0$ curves which are taken from Ref. 7 represent longitudinal compression with the transverse edges held in place. In Fig. 7, the prebuckling part of the $\bar{v}=0$ curve is represented by loading along a radial line where N_y builds up linearly with N_x until buckling. Buckling occurs at a lower value of N_x because of the presence of N_y. The initial postbuckling slope for the $\bar{v}=0$ curves in Figs. 5 and 6 is about one-half the prebuckling slope indicating a loss of stiffness, and in the postbuckling range the slope decreases slightly with change in wavelength of the buckles. The curves for $\bar{v}$ not equal to zero have been calculated for the present paper. The $\bar{v}=4\bar{v}_{cr}$ curve for isotropic plates and the $\bar{v}=7\bar{v}_{cr}$ for the ±45° laminated plate are always in the postbuckling range for $\bar{u}$ in compression. Except for the prebuckling range, these curves follow the trends of the $\bar{v}=0$ curve and give slightly lower N_{xav} values for part of the range. The curves for $\bar{v}=20\bar{v}_{cr}$ fall below the curve for $\bar{v}=4\bar{v}_{cr}$ for the isotropic plate and above the curve for $\bar{v}=7\bar{v}_{cr}$ for the ±45° laminated plate. Also shown on these figures are results taken from Ref. 6 for the edges straight but free of stress on the average $N_{yav}=0$. The case for $N_{yav}=0$ has a slightly higher buckling load than the $\bar{v}=0$ case but slightly lower postbuckling slope. These figures show that under combined longitudinal and transverse compression, the average longitudinal-stress resultant is not affected very much either by specifying the transverse edge displacement or by requiring that the average transverse stress resultant is zero.

The average transverse-stress resultant N_{yav} of a long plate in combinations of applied compressive longitudinal and transverse displacements $\bar{u}$ and $\bar{v}$ is given in Fig. 7 for an isotropic plate. N_{yav} is plotted vs $\bar{v}$ for different values of $\bar{u}$. A similar plot is shown in Fig. 8 for a ±45° laminated composite plate. In the figures, N_{yav} is normalized by N_{ycr}, the stress resultant at buckling when only N_y is acting, and $\bar{u}$ and $\bar{v}$ are normalized by the corresponding displacements at buckling $\bar{u}_{cr}$ and $\bar{v}_{cr}$. The $\bar{u}=0$ curves represent transverse compression with the longitudinal edges held in place. In Fig. 3 the prebuckling part of the curves for $\bar{u}=0$ in Figs. 7 and 8 represents a loading along a radial line which intersects with the vertical line. Buckling occurs at the same value of N_y (at the vertical line) but at a lower value of $\bar{v}$ because of the presence of N_x. The initial postbuckling slope for the $\bar{u}=0$ case for an isotropic plate (Fig. 7) is about one-half while the initial postbuckling slope for the ±45° laminated plate (Fig. 8) is about two-thirds. For $\bar{u}>1$, the postbuckling slopes increase for the isotropic plate but N_{yav} becomes negative (Fig. 7) for small $\bar{v}$; that is, the average transverse-stress resultant becomes tensile for small $\bar{v}$. The postbuckling slopes remain about the same for the ±45° laminated plate, Fig. 8, and N_{yav} remains in compression. The wavelengths are longer along the $\bar{u}=0$ curve, especially for smaller $\bar{v}$, and the trends of the $\bar{u}=0$ curves differ from the trends in the other curves in this range. This effect is more pronounced for the ±45° laminate (see Fig. 8). Also shown in Figs. 7 and 8 are the plate-column curves which hold when the long ends are free to expand (i.e., $N_{xav}=0$). These curves indicate that the plate-column has no stiffness in the postbuckling range. The plate-column curves are very different in character as compared to the curves which apply when $\bar{u}$ is controlled.

Combined Transverse Compression and Shear

The average shear-stress resultant N_{xyav} of a long plate loaded in combinations of applied transverse compression and applied shear displacements $\bar{v}$ and $\bar{u}_{sh}$, respectively, is given in Fig. 9 for an isotropic plate. N_{xyav} is plotted vs $\bar{u}_{sh}$ for different values of $\bar{v}$. A similar plot is shown in Fig. 10 for a ±45° laminated composite plate. In the figures, N_{xyav} is normalized by N_{xycr}, the stress resultant at buckling when only N_{xy} is acting, and $\bar{v}$ and $\bar{u}_{sh}$ are normalized by the corresponding displacements at buckling $\bar{v}_{cr}$ and $\bar{u}_{shcr}$. The $\bar{v}=0$ curves which are taken from Ref. 7 represent shearing with the transverse edges held apart the same distance as before loading (note, also, that $\bar{u}=0$). In Fig. 4, the prebuckling parts of the $\bar{v}=0$ curve can be represented by a vertical line along the ordinate with $N_y=0$. The initial postbuckling slope for the $\bar{v}=0$ curves in Figs. 9 and 10 is almost the same as the prebuckling slope indicating that there is only a slight reduction in stiffness immediately after buckling. For $\bar{v}\neq 0$, the results of the present analysis for this case are not much different than the $\bar{v}=0$ case. For the isotropic case (see Fig. 9), the curves decrease slightly in slope with increase in $\bar{v}$ but the curves are close together. For the ±45° laminate (see Fig. 10), the curves appear to be parallel and more spread

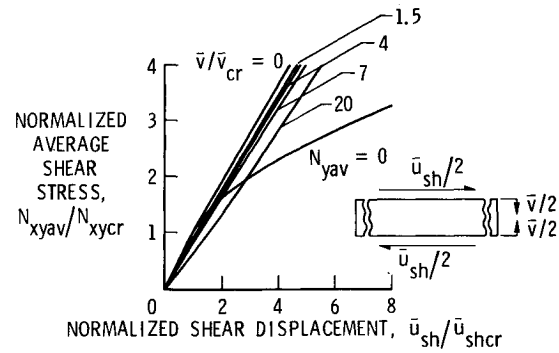

Fig. 9 Average shear stress for a long isotropic plate in combined shear and transverse compression.

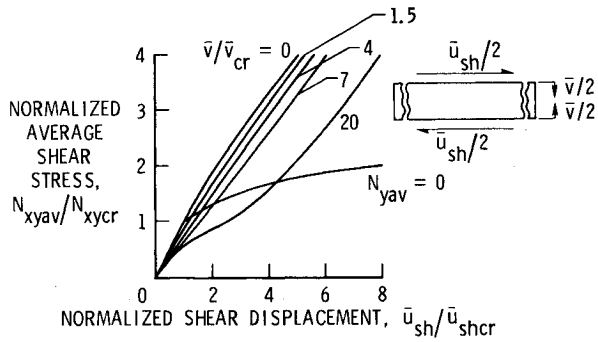

Fig. 10 Average shear stress for a long ±45° laminated composite plate in combined shear and transverse compression.

out but there is a change in the shape of the curves for small $\bar{u}_{sh}$ where the wavelength is large. Also shown in Figs. 9 and 10 is a curve taken from Ref. 6 where the edges were free to move in (i.e., $N_{yav} = 0$) but still remain straight. The curves for $N_{yav} = 0$ are quite different than those for controlled $\bar{v}$ and generally indicate much lower prebuckling stiffness.

The average transverse compressive-stress resultant N_{yav} of a long plate loaded in combinations of applied transverse compression and applied shear displacements $\bar{v}$ and $\bar{u}_{sh}$, respectively, is given in Fig. 11 for an isotropic plate, N_{yav} is plotted vs $\bar{v}$ for different values of $\bar{u}_{sh}$. A similar plot is shown in Fig. 12 for a ±45° laminated composite plate. In the figures, N_{yav} is normalized by N_{ycr}, the stress resultant at buckling when only N_y is acting, and $\bar{v}$ and $\bar{u}_{sh}$ are normalized by the corresponding displacements at buckling $\bar{v}_{cr}$ and $\bar{u}_{shcr}$. The $\bar{u}_{sh} = 0$ curve represents the behavior of the plate in transverse compression (when the ends are held in place, i.e., $\bar{u} = 0$); these curves also appear in Figs. 7 and 8. Both sets of curves indicate high tensile stresses for low $\bar{v}$. The slopes of the curves indicate that the stiffness in the transverse direction of the ±45° laminate increases more with an increase in $\bar{v}$ than it does for the isotropic plate. Both sets of curves have a change in pattern trend where $\bar{u}_{sh}$ is small and the wavelengths are long.

The average longitudinal compressive-stress resultant N_{xav} of a long plate loaded in combinations of applied transverse compression and applied shear displacements $\bar{v}$ and $\bar{u}_{sh}$, respectively, is given in Fig. 13 for an isotropic plate. N_{xav} is plotted vs $\bar{v}$ for different values of $\bar{u}_{sh}$. A similar plot is shown in Fig. 14 for a ±45° laminated composite plate. In the figures, N_{xav} is normalized by N_{xcr}, the stress resultant at buckling when only N_x is acting, and $\bar{v}$ and $\bar{u}_{sh}$ are normalized by the corresponding displacements at buckling $\bar{v}_{cr}$ and $\bar{u}_{shcr}$. The longitudinal average stresses that appear for this problem are all in tension. For the isotropic plate (Fig. 13), the average stresses are independent of the transverse displacement. For the ±45° laminate (Fig. 14), the longitudinal average tensile stresses decrease with increase of

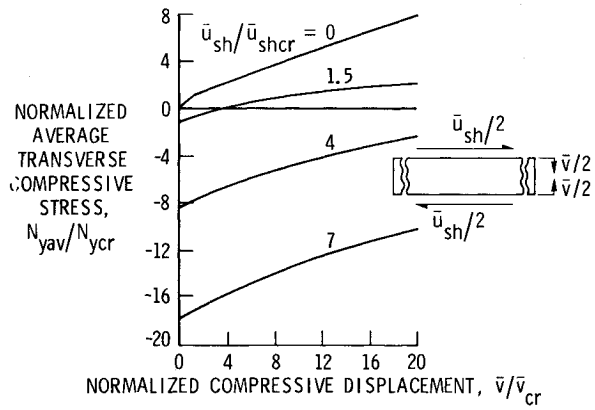

Fig. 11 Average transverse shear for a long isotropic plate in combined shear and transverse compression.

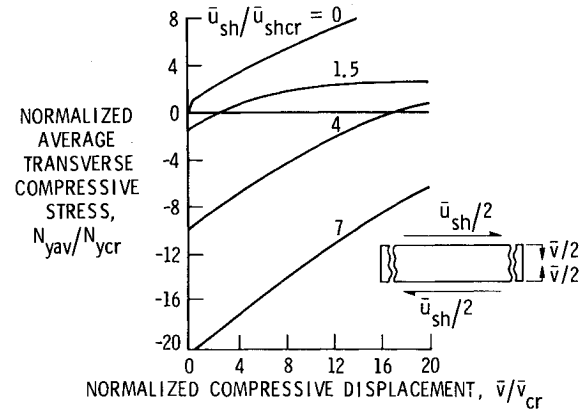

Fig. 12 Average transverse stress for a long ±45° laminated composite plate in combined shear and transverse compression.

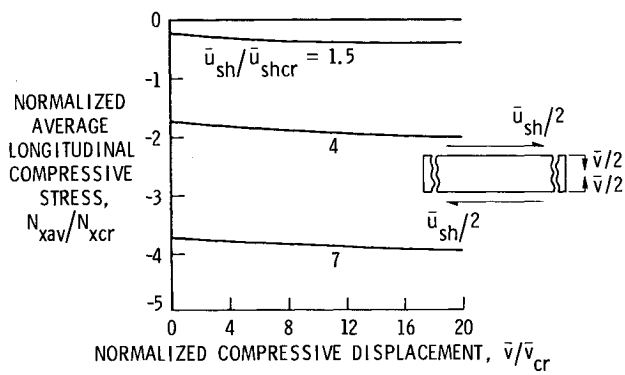

Fig. 13 Average longitudinal stress for a long isotropic plate in combined shear and transverse compression.

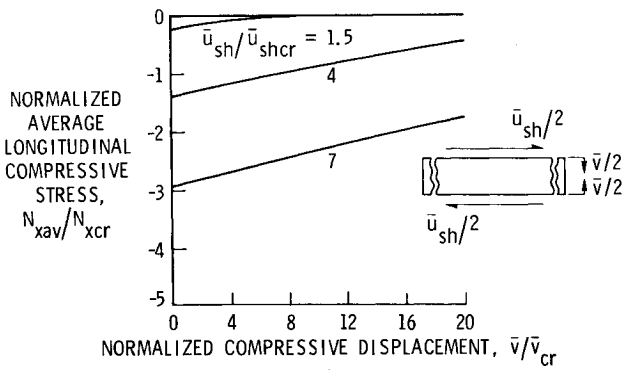

Fig. 14 Average longitudinal stress for a long ±45° laminated composite plate in combined shear and transverse compression.

transverse loading for higher values of the shear displacement.

Concluding Remarks

Postbuckling results are presented for long simply supported isotropic and ±45° composite plates under two combined load cases. The first combined load case considered involves combinations of applied compressive longitudinal and transverse displacements. For much of the postbuckling range considered, the longitudinal stress decreased slightly with increase in transverse compression, but, generally, the longitudinal stress was not affected by the presence of the transverse compression. The transverse stress, however, was affected significantly by the presence of longitudinal compression. If the longitudinal stress is zero as in the plate-column case, the postbuckling slope of the characteristic load-shortening curve of the plate is essentially zero. If the longitudinal displacement is zero for the isotropic plate, the initial postbuckling slope is about one-half of the prebuckling slope. If the longitudinal displacement is zero for the ±45° laminated composite plate, then the initial postbuckling slope is about two-thirds. With change in wavelength, the postbuckling slope ratio decreases to about one-half. With increases in applied longitudinal displacements, the isotropic plate increases in stiffness (slope) while the ±45° laminated plate maintains its slope of about one-half.

The other combined load case considered involves combinations of applied transverse compression and applied shear displacements. For the transverse compression cases treated, the postbuckling slopes of the curves indicate that the postbuckling stiffness in shear is very high. Previous results based on stress-free edges gave much lower stiffnesses. High tensile stresses in the transverse and longitudinal directions appear and generally decrease with increase in transverse load. One exception is the isotropic plate for which the average longitudinal stresses remain constant with increase in transverse load.

The trends of the curves differ in the range where the wavelengths are longer. For the case of combined longitudinal and transverse compression this difference in trends occurs for small applied longitudinal displacement, and for the case of combined transverse compression and shear this difference occurs for small shearing. The difference in the trends of the curves is more pronounced for the ±45° laminated composite plate than for the isotropic plate.

References

[1]Stowell, E. Z. and Schwartz, E. B., "Critical Stress for an Infinitely Long Flat Plate with Elastically Restrained Edges under Combined Shear and Direct Stress," NACA ARR 3K13, 1943.

[2]Batdorf, S. B., Stein, M., and Libove, C., "Critical Combinations of Longitudinal and Transverse Direct Stress for an Infinitely Long Flat Plate with Edges Elastically Restrained Against Rotation," NACA ARR L6A05a, 1946.

[3]Batdorf, S. B. and Houbolt, J. C., "Critical Combinations of Shear and Transverse Direct Stress for an Infinitely Long Flat Plate with Edges Elastically Restrained Against Rotation," NACA ARR L4L14, 1945.

[4]Almroth, B. O. and Brogan, F. A., "The STAGS Computer Code," NASA CR 2950, 1978.

[5]Stein, M., "Postbuckling of Orthotropic Composite Plates Loaded in Compression," *AIAA Journal*, Vol. 21, Dec. 1983, pp. 1729-1735.

[6]Stein, M., "Postbuckling of Long Orthotropic Plates in Combined Shear and Compression," AIAA Paper 83-0876, 1983.

[7]Stein, M., "Analytical Results for Postbuckling Behavior of Plates in Compression and in Shear," NASA TM 85766, March 1984; *Aspects of the Analysis of Plate Structures*, to be published.

[8]Lentini, M. and Pereyra, V., "An Adaptive Finite Difference Solver for Nonlinear Two-Point Boundary Problems with Mild Boundary Layers," *SIAM Journal of Numerical Analysis*, Vol. 14, March 1977, pp. 91-111.

[9]Stein, M., "Loads and Deformations of Buckled Rectangular Plates," NASA TR R-40, 1959.